JOURNAL OF GEOPHYSICAL RESEARCH, VOL. 88, NO. C9, PAGES 5191–5202, JUNE 20, 1983

CO_2 Radiative Parameterization Used in Climate Models: Comparison With Narrow Band Models and With Laboratory Data

J. T. KIEHL AND V. RAMANATHAN

National Center for Atmospheric Research, Boulder, Colorado 80307

Absorptances for the 15-μm band system of CO_2 are calculated from three models: the Goody model, the Malkmus model, and a wide band formulation. The wide band formulation used in this study explicitly accounts for hot and isotopic bands of CO_2. Comparison is made between these calculated absorptances and measured absorptances. The band models are in good agreement with the measured absorptances. The sensitivity of these models to increased CO_2 is investigated by intercomparing flux and heating rate changes computed by the three models. It is concluded that little difference exists between the narrow band and the wide band absorptance models, provided the wide band models account explicitly for the various hot and isotopic bands of CO_2. We show that significant errors result if the Goody or Malkmus model is applied to spectral intervals larger than 10 cm^{-1}. Thus, our results suggest that climate models that employ Goody or Malkmus type models with coarser spectral resolution (>10 cm^{-1}) may be subject to errors (in CO_2 fluxes and heating rates) larger than 10%. We also show the differences between the narrow and the wide band model treatment of H_2O-CO_2 overlap in the 15-μm region. The H_2O continuum absorption in the 15-μm region alters significantly the vertical distribution of CO_2 heating in the lower troposphere.

1. INTRODUCTION

Over the years many methods have been developed to calculate the absorption of infrared radiation by molecules. In particular, two general classes of techniques have become popular for the treatment of molecular absorption. Both of these techniques are employed in climate models, and, therefore, comparison of these two methods with each other and with experimentally measured absorptance is of great value. We have chosen CO_2 for our comparison study because of the potential climatic effects of increased CO_2 and because a systematic study such as the present one has not been attempted for validating the CO_2 parameterizations used in climate models.

The first technique is commonly referred to as the 'narrow band' method. This approach was initiated by the work of *Goody* [1952] and *Malkmus* [1967] and has been applied to both remote sensing studies and climate modeling [*Hunt and Mattingly*, 1976; *Ellingson and Gille*, 1978; *Gille*, 1973; *Groves and Tuck*, 1980; *Haigh and Pyle*, 1979, to name a few].

The radiant exitance at the top of the atmosphere computed by the narrow band method in the 12–18 μm region is in excellent agreement with satellite measurements [*Ellingson and Gille*, 1978]. As discussed in the next section, the narrow band method assumes random distribution of rotational lines within each narrow spectral interval. Hence, it is somewhat surprising that this method is in such good agreement for CO_2, which has regular lines (i.e., the mean line spacing is approximately uniform within a band). The main reason for the success of the narrow band method that employs the random line assumption can be attributed to the fact that CO_2 has many hot and isotopic bands, such that within each narrow spectral interval the lines due to these bands are randomly distributed.

The second approach to calculating band absorptance is known as the 'broad' or 'wide band' formulation and was first used by *Edwards and Menard* [1964], *Goody and Belton* [1967], and later by *Cess and Ramanathan* [1972].

Each of these approaches have particular advantages. The narrow band models incorporate the detailed spectral structure over narrow spectral intervals and thus allow one to calculate spectral radiances. The wide band method allows one to calculate the absorptance of an entire band and are useful for climate model studies, where calculations are repeated many times. The question that we address in the present study is, How well do these two approaches compare with experimentally measured absorptances and with each other? We have chosen three specific band models in order to answer this question. Narrow band absorptances are calculated with the Goody model and the Malkmus model. Wide band absorptances are calculated from a formulation based on the work of *Cess and Ramanathan* [1972] and *Ramanathan* [1976].

The present study is limited to the 15-μm band system of CO_2. Table 1 lists the vibrational transitions that are included in the present study. We have chosen this spectral region for two reasons. First, the detailed experimental measurements of absorptance for this band due to *Gryvnak et al.* [1976] facilitates comparison of calculated absorptances with measured absorptances. Second, this band system is the most important for studying flux changes due to increased CO_2, a problem that we address in the following sections. Among several available laboratory measurements, *Gryvnak et al.* [1976] were chosen for our study for the following reasons: (1) these are the most recent measurements for the 15-μm band system; (2) the range of CO_2 path lengths and total pressures chosen by *Gryvnak et al.* [1976] are sufficiently close to those encountered in the atmosphere that they enable this comparison study relevant for the CO_2 problem.

The study is presented in six sections. Section 2 reviews the three band models used to calculate band absorptances. Section 3 presents the comparison of the three models with experimentally measured absorptances for a wide range of temperatures, absorber pressures, and amounts. We also

Paper number 3C0372.
0148-0227/83/003C-0372$05.00

TABLE 1. Band Parameters Used in the Wide Band Formulation of Equation (A1).

Band Number	Band Center, ν_j, cm^{-1}	Transition,* $v_1v_2^lv_3 \rightarrow v_1'v_2''^{l''}v_3'$	Strength at 300 K, cm^{-2} atm^{-1}	Lower State, E_j, cm^{-1}	Mean Line Spacing,† d_{ij}, cm^{-1}
1	667.381	00^00–01^10	194.0	0.0	1.56
2	618.029	01^10–(10^00)II	4.27	667.381	1.56
3	720.805	01^10–(10^00)I	5.0	667.381	1.56
4	667.751	01^10–02^20	15.0	667.381	0.78
5	647.063	(10^00)II–(11^10)II	0.7	1285.410	1.56
6	791.446	(10^00)II–(11^10)I	0.022	1285.410	1.56
7	597.342	02^20–(11^10)II	0.14	1335.131	0.78
8	741.724	02^20–(11^10)I	0.144	1335.131	0.78
9	668.107	02^20–03^30	0.85	1335.131	0.78
10	544.288	(10^00)I–(11^10)II	0.01	1388.185	1.56
11	668.670	(10^00)I–(11^10)I	0.3	1388.185	1.56
12	652.529	(11^10)II–(12^20)II	0.045	1932.473	0.78
13	720.286	(11^10)I–(20^00)I	0.005	2076.855	1.56
14	615.887	(11^10)II–(20^00)III	0.015	1932.473	1.56

Band parameters in columns two through five are from *Drayson* [1973].
*Roman numerals identify levels in Fermi resonance.
†For $C^{12}O^{16}O^{18}$ and $C^{12}O^{16}O^{17}$ the mean line spacing is 0.78 for all bands.

show the strong dependence of the narrow band model results on the width of the spectral interval. Section 4 compares radiative fluxes and heating rates calculated from the narrow and wide band models for three temperature profiles representative of low, mid, and high latitudes. Section 5 addresses the problem of water vapor overlap in the 15-μm band region. Section 6 discusses the implications of our findings to climate modeling.

2. Theory of Narrow and Wide Band Models

2.1. *Narrow Band Models*

The band absorptance is defined as

$$A(P, w, T) = \int_{-\infty}^{\infty} A_\nu(P, w, T)\, d\nu \tag{1}$$

where P, w, T are the total pressure, absorber amount, and absolute temperature. A_ν is the monochromatic absorption at the wave number ν. Calculation of the band absorptance from the monochromatic absorption is computationally prohibitive for climate model studies. For these calculations, therefore, a narrow band absorptivity has been defined. The absorptivity for a spectral interval $\Delta\nu$ is related to the transmissivity by

$$A_{\Delta\nu}(P, w, T) = 1 - T_{\Delta\nu}(P, w, T) \tag{2}$$

Goody [1952] showed that the transmissivity for a given narrow spectral interval, $\Delta\nu$, due to overlapping collision broadened lines could be represented by

$$T_{\Delta\nu} = \exp\left\{-\left(\frac{s}{\delta}\right)_{\Delta\nu} w\left[1 + \left(\frac{s}{\pi\alpha}\right)_{\Delta\nu} w\right]^{-1/2}\right\} \tag{3}$$

where s is the mean line strength for the interval, α is the mean line half-width, and δ is the mean line spacing. Goody's model assumes that the line strengths within the interval $\Delta\nu$ are distributed exponentially. However, as was pointed out by *Yamamoto and Sasamori* [1957] and *Malkmus* [1967], there exists no a priori justification for the lines in a particular interval to be distributed in this manner. Malkmus has pointed out that many molecular vibration-rotation spectra contain a large number of weak lines. Thus, the exponential distribution does not weight these lines correctly. Introducing a s^{-1} dependence to the line distribution, *Malkmus* [1967] derived the transmissivity to be

$$T_{\Delta\nu}(P, w, T) = \exp\left\{-\frac{(s/\delta)_{\Delta\nu}}{2(s/\pi\alpha)_{\Delta\nu}} \cdot \left[(1 + 4w(s/\pi\alpha)_{\Delta\nu})^{1/2} - 1\right]\right\} \tag{4}$$

where the line parameters are the same as those used in the Goody model.

We have calculated the line parameters from the line data of *McClatchey et al.* [1973]. The spectral parameters used for the calculations of section 3 were based on a band interval of 560–780 cm^{-1} with $\Delta\nu = 5$ cm^{-1}. This total band width agrees with the experimental limits of *Gryvnak et al.* [1976]. *Robertson et al.* [1981] have found excellent agreement between transmissivities calculated with a high resolution model (0.02 cm^{-1}) and 5 cm^{-1} averaged band model. For the calculations for sections 4 and 5 we used a total interval 500–800 cm^{-1}, which agrees with intervals used by other investigators. We use the most current version of the line data available from AFGL. The line strength parameters of carbon dioxide and water vapor at a temperature of 235 K for this spectral interval are shown in Figure 1. Temperature dependence of the line parameters is treated by the method described by *Rodgers and Walshaw* [1966].

2.2. *Wide Band Model*

The wide band formulation, based on the work of *Edwards and Menard* [1964], assumes that each band can be expressed in terms of the following band parameters: a dimensionless optical depth, u; mean line-width parameter, β; and the effective bandwidth parameter, A_0; which are defined as

$$u = \frac{Sw}{A_0} \tag{5a}$$

$$\beta = \frac{4\gamma}{d} \tag{5b}$$

where S is the band strength, w is the amount of gas, γ is the

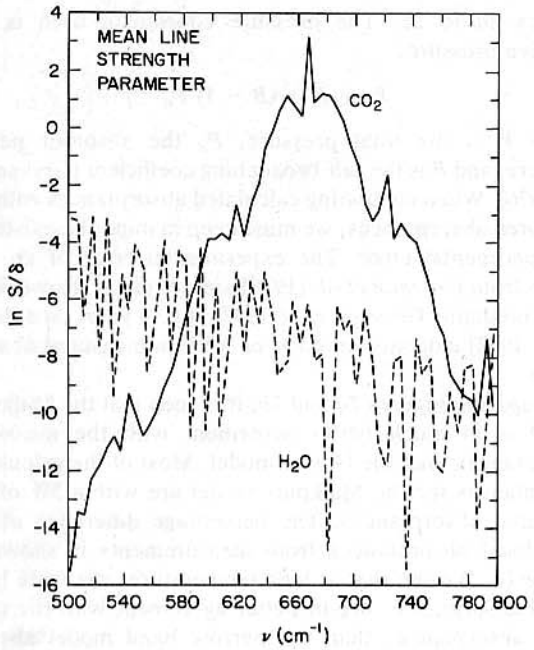

Fig. 1. Random model mean line strength parameters, S/δ, at a temperature of 235 K, for CO_2 and H_2O for $\Delta\nu = 5$ cm^{-1}.

mean line width for the band, and d is the mean line spacing. *Edwards and Menard* [1964] showed that the band absorptance, A (equation (1)), for a nonrigid rotator molecule asymptotes to the following limits,

For $\beta \ll 1$

$$A = A_0 u \qquad u \ll 1 \qquad u/\beta \ll 1 \tag{6a}$$

$$A = 2A_0\sqrt{u\beta} \qquad u/\beta \gg 1 \qquad \beta u \ll 1 \tag{6b}$$

$$A = A_0 \ln u\beta \qquad u \gg 1 \tag{6c}$$

For $\beta \gg 1$

$$A = A_0 u \qquad u \ll 1 \tag{7a}$$

$$A = A_0 \ln u \qquad u \gg 1 \tag{7b}$$

The $\beta \ll 1$ limit applies where individual rotational lines within a band are nonoverlapping, while the $\beta \gg 1$ limit refers to the case when the lines are so broad that the overlap of the neighboring lines smears out the line structure such that, as shown in equations (7a)–(7b), the band absorptance is independent of the line structure [see also *Cess and Tiwari*, 1972]. Equations (6a) and (7a) are the linear or optically thin limit; (6b) is the square root limit and applies when the mean line center optical depth, u/β, is large but the individual lines are nonoverlapping, i.e., $\beta \ll 1$, and hence this limit is also referred to as the strong nonoverlapping line limit.

Goody and Belton [1967], using a suggestion of *Yamamoto and Sasamori* [1957], proposed that the absorptance of the 15-μm CO_2 band could be expressed as

$$A = 2A_0 \ln\left[1 + \frac{u}{\sqrt{4 + u/\beta}}\right] \tag{8}$$

As pointed out by *Cess and Tiwari* [1972], (8) does not asymptote to the proper limit for $\beta \gg 1$ and $u \gg 1$ (see (7b)).

Cess and Ramanathan [1972] modified (8) such that all of the asymptotic limits ((6) and (7)) are satisfied, and their expression was extended by *Ramanathan* [1976] to account for the hot and isotopic bands of CO_2, as follows:

$$A = 2A_0 \ln\left[1 + \sum_{i=1}^{4}\sum_{j=1}^{14} \frac{u_{ij}}{[4 + u_{ij}(1 + 1/\beta_{ij})]^{1/2}}\right] \tag{9}$$

where the summations are over isotopes, i, and bands, j (j = 1, fundamental, $j > 1$, hot bands). This expression is strictly valid for completely overlapped bands. As discussed later, (9) is modified slightly to account for the partially overlapping CO_2 bands in the 15-μm region. The subscript j should not be confused with the rotational quantum number traditionally used in the spectroscopic literature, and

$$u_{ij} = q_i \int \frac{S_j(T)}{A_0(T)} P_a \, dz \tag{10}$$

$$\beta_{ij} = \frac{4}{d_{ij}u_{ij}} \int \gamma(T)P \, du_{ij} \tag{11}$$

where $S_j(T)$ is the band strength of $C^{12}O_2{}^{16}$ at temperature T, in cm^{-2} atm^{-1}, q_i is the isotopic abundance relative to $C^{12}O_2{}^{16}$. It should be noted that the isotopic band strengths are calculated by multiplying the band strengths of $C^{12}O_2{}^{16}$ by the isotopic abundances relative to $C^{12}O_2{}^{16}$, as suggested by *Drayson* [1973] (i.e., in (10), q_iS_j yields the band strength of the various isotopic bands). Some investigators choose to list these bands separately. The relative isopotic abundances for $C^{12}O_2{}^{16}$, $C^{13}O_2{}^{16}$, $C^{12}O^{16}O^{18}$, and $C^{12}O^{16}O^{17}$ were obtained from *Drayson* [1973] ($q_1 = 1.0$, $q_2 = 1.12 \times 10^{-2}$, $q_3 = 4.08 \times 10^{-3}$, $q_4 = 7.42 \times 10^{-4}$). Z is the path distance in cm, P_a is the absorber pressure, d_{ij} is the mean line spacing, and γ is the mean line half-width which is assumed to be the same for all bands. The four quantities that must be specified for a given band are S_j, γ, d_{ij}, and A_0.

The temperature dependence of the band strengths is determined from [*Penner*, 1959; *Madden*, 1961]

$$S_j(T) = S_j(T_0)\left(\frac{T_0}{T}\right)\frac{Q_v(T_0)}{Q_v(T)}\frac{\{1 - e^{-1.439\,\nu_j/T}\}}{\{1 - e^{-1.439\,\nu_j/T_0}\}} \cdot \exp\{1.439E_j[1/T_0 - 1/T]\} \tag{12}$$

where $S_j(T_0)$ is the band strength at reference temperature T_0, Q_v is the vibrational partition function, ν_j (cm^{-1}) is the band center, and E_j (cm^{-1}) is the energy of the lower level. The fourth expression on the right-hand side of (12) accounts for stimulated emission. The last term is a Boltzmann factor, which accounts for the population of higher vibrational transitions (hot bands). We assume that the CO_2 molecule behaves as a harmonic oscillator; then, the vibrational partition function is given by *Herzberg* [1945],

$$Q_v(T) \approx (1 - e^{-1.439\,\nu_j/T})^{-2}$$

We adopt the band strengths tabulated by *Drayson* [1973] for the reference temperature of 300 K. For each isotope, we employ 14 bands for the present calculations, and, thus, our calculations include a total of 56 CO_2 bands in the 12–18 μm region. Band parameters for the $C^{12}O_2{}^{16}$ isotope are listed in Table 1. We have also performed calculations that include all

19 bands listed by *Drayson* [1973] for $C^{12}O_2{}^{16}$. Differences in absorptances between these calculations and those employing the 14 bands of $C^{12}O_2{}^{16}$ listed in Table 1 were negligible (<0.5%).

The mean line width was determined from the line parameters of *Yamamoto et al.* [1969], as follows:

$$\gamma = \frac{\left[\sum_{l=0}^{\infty} \sqrt{\gamma_l s_l}\right]^2}{\left[\sum_{l=0}^{\infty} \sqrt{s_l}\right]^2} \tag{13}$$

where γ_l and s_l are the half-width and intensity of individual rotational lines within the band and γ is the half-width for the whole band. Employing γ_l from *Yamamoto et al.* [1969], Cess and Ramanathan computed γ from (13) for a pure CO_2 atmosphere and *Ramanathan* [1976] accounted for nitrogen broadened CO_2 lines and obtained

$$\gamma(T) = 0.067(300/T)^{2/3}(\text{cm}^{-1}) \tag{14}$$

which is used for the calculations reported in this study. Note that in (11) the value of γ as given by (14) is used for all of the bands. Depending on the band type, the mean line spacing, d_{ij}, is either $4B$ or $2B$ (see Table 1), where B is the rotational constant of CO_2, 0.39 cm^{-1}.

The effective bandwidth parameter, $A_0(T)$, must be determined from measurements of total band absorptance, in conjunction with the asymptotic expression (6*c*) and (7*b*). From (6*c*) and (7*b*),

$$\frac{\partial A}{\partial \ln u} = A_0 \qquad u \gg 1 \tag{15}$$

and, hence, A_0 is obtained from measurements as the slope of A with respect to ln u. For A_0, we use *Edwards and Menard* [1964] value given by

$$A_0 = 22.18(T/296)^{1/2}\ (\text{cm}^{-1}) \tag{16}$$

The temperature dependence of A_0, which can also be derived theoretically [see *Edwards and Menard*, 1964; *Cess and Tiwari*, 1972], accounts for the effective increase in the bandwidth with increasing temperature (i.e., as temperature increases, the number of molecules in the higher rotational quantum levels increases, which enhances the absorption by the wings of the band). It is important to note that the value of A_0 given in (16) was obtained from a data set different from that of *Gryvnak et al.* [1976]. This value of A_0 is fixed for all calculations and is not used to tune the calculated absorptances.

Equation (9) is an expression for the absorptance of totally overlapped bands. However, six of the band systems listed in Table 1 are not strongly overlapped, namely the 544.288, 597.342, 618.029, and 615.887; 720.286; and 720.805, 741.724, and 791.446 cm^{-1} bands. The band absorptance expression for these partially overlapped bands is discussed in the appendix.

3. Comparison of Narrow and Wide Band Absorptances With Measured Absorptances

The percent difference between the calculated and 30 measured absorptances for a wide range of pressures and absorber amounts at a temperature of 310 K are shown in Figures 2*a* to 2*c*. The pressure coordinate used is the effective pressure,

$$P_e = P + (B - 1)\,P_a \tag{17}$$

where P is the total pressure, P_a the absorber partial pressure, and B is the self-broadening coefficient [*Gryvnak et al.*, 1976]. When comparing calculated absorptances with the measured absorptances, we must keep in mind the existence of experimental error. The experimental error of absorptances from *Gryvnak et al.* [1976] are not given. However, a study predating *Gryvnak et al.* [1976] by 14 years [see *Burch et al.*, 1962] indicates an error of ±5% in measured absorptances.

Comparing Figures 2*a* and 2*b*, it is seen that the Malkmus model is in much better agreement with the measured absorptances than the Goody model. Most of the calculated absorptances for the Malkmus model are within 5% of the measured absorptances. The percentage difference of the wide band absorptances from measurements is shown in Figure 2*c*. We see that at high temperatures the wide band model absorptances are in better agreement with the measured absorptances than the narrow band model absorptances.

Comparisons between calculated absorptances and 21 measured absorptances of *Edwards* [1960] are shown in Figures 3*a* to 3*c*. *Edwards* [1960] data are for a temperature of 294 K and for relatively large pressures and amounts of CO_2. We present this data not because they are relevant to terrestrial conditions but because they illustrate how well the models do for rather extreme conditions. The calculations agree with measured values within 9% (with minor exceptions).

Comparisons between calculated absorptances and the measured absorptances of *Gryvnak et al.* [1976] for temperatures of 274 K and 244–246 K are shown in Figures 4 and 5, respectively. A total of 16 data points were employed for the comparison at a temperature of 274 K, while 24 data points were used for the comparison at temperatures of 244–246 K. These figures indicate that the models are in excellent agreement with the measured absorptances. We see, once again, that at 274 K the narrow band model absorptances are larger than the measured absorptances for all pressures and amounts, whereas at lower temperatures they can be larger or smaller than measured absorptances. The wide band absorptances are greater and less than the measured absorptances for certain amounts and pressures. Overall, the Malkmus narrow band model and the wide band model are in excellent agreement with the data.

There is no a priori method to determine the size of the spectral interval for the narrow band models. To determine how sensitive the calculated absorptances are to a given spectral interval, we have calculated absorptances with the Malkmus model for four spectral widths. The results of these calculations for spectral intervals of $\Delta\nu$ = 5, 20, 40, and 80 cm^{-1}, respectively, are shown in Figures 6*a* to 6*d*. We compare all calculated absorptances with the absorptances obtained from a spectral interval of $\Delta\nu$ = 2 cm^{-1}, since this interval resulted in absorptances which were in excellent agreement with the measured absorptances at a temperature of 310 K. The results from Figure 6*a* indicate that very little difference exists if an interval of 5 cm^{-1} is used instead of 2 cm^{-1}, and those from Figure 6*b* indicate that errors of the order of 10% can be expected if an interval size of 20 cm^{-1} is

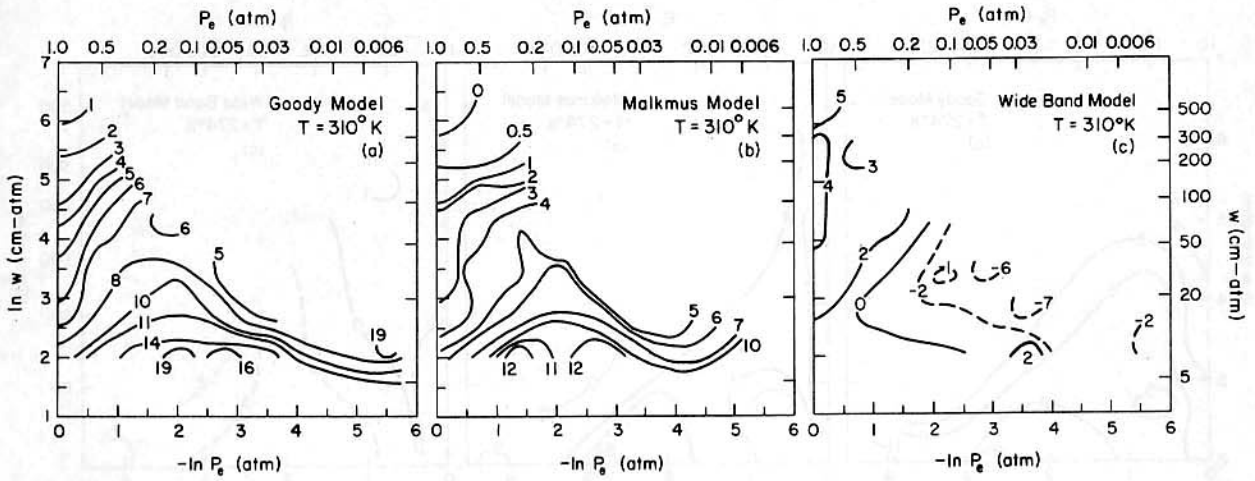

Fig. 2. Comparison of theoretical band absorptances with 30 measured absorptances of *Gryvnak et al.* [1976] at a temperature of 310 K. Contours represent percentage difference of calculated from measured absorptances for various CO_2 amount, w, and effective pressures, P_e, for the (*a*) Goody model, (*b*) Malkmus model, (*c*) wide band model.

chosen. Errors of the order of 15% can be expected if the interval is 40 cm^{-1} as evidenced by Figure 6*c*. Finally, the case of an interval size of 80 cm^{-1} is shown in Figure 6*d*. Errors of the order of 25% can be expected for this large interval. The reason the error is growing as the spectral interval increases is that we are trying to fit the absorptance due to a complex band structure by a limited number of parameters. If the interval were chosen to be 220 cm^{-1}, then we would essentially be attempting to fit the entire band system by two parameters. This method is not comparable to the wide band model described in section 2.2. The wide band model described in that section uses band parameters for each of the bands present in the spectral interval from 560 to 780 cm^{-1}. In other words, each band, be it the fundamental band or a hot band or an isotopic band, is treated in detail. The effects of using wide spectral intervals on the sensitivity of model results is discussed in section 4.

4. Radiative Fluxes and Heating Rates

The radiative fluxes defined in terms of the band absorptance for a pure CO_2 atmosphere are

$$F^{\uparrow} = \sigma T_s^4 - \tilde{B}_{15}(T_s)A(|u - u_0|) - \int_{u_0}^{u} \tilde{B}_{15}[T(u')]\, dA(|u - u'|) \tag{18}$$

$$F^{\downarrow} = -\int_{0}^{u} \tilde{B}_{15}(u')\, dA(|u - u'|) \tag{19}$$

where T_s is the temperature at the surface, $\tilde{B}_{15}(T)$ is the Planck function evaluated at the band center of 667.4 cm^{-1}, and σ is the Stefan-Boltzmann constant. The optical depth, u (see, equation (10)), is measured from the top of the atmosphere, with u_0 the optical depth of the entire atmosphere and $u = 0$ denotes the top of the atmosphere. The optical depth u now includes a factor of 1.66 to account for the angular integration over isotropic radiation. We have assumed a mean Planck function evaluated at the band center for the narrow band calculations also. We investigated this assumption by including the wave number dependence of the Planck function in our flux calculations and determined that

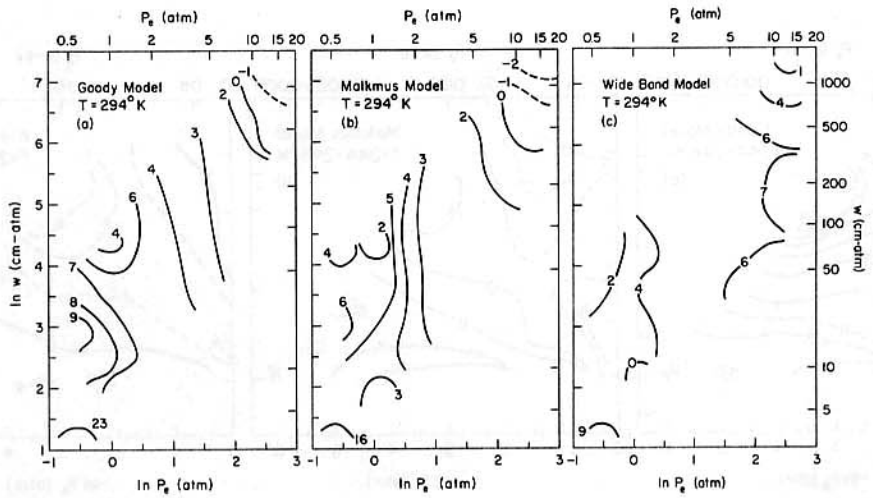

Fig. 3. Comparison of theoretical band absorptances with 21 measured absorptances of *Edwards* [1960] at a temperature of 294 K. Contours represent percentage difference of calculated from measured absorptances for various CO_2 amounts, w, and effective pressures, P_e, for the (*a*) Goody model, (*b*) Malkmus model, (*c*) wide band model.

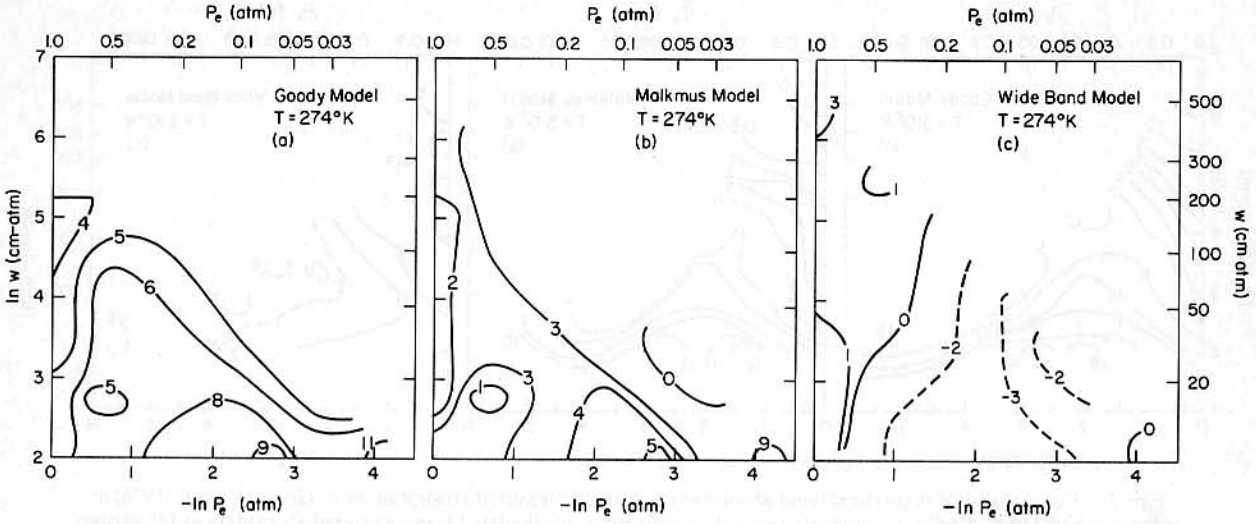

Fig. 4. Comparison of theoretical band absorptances with 16 measured absorptances of *Gryvnak et al.* [1976] at a temperature of 274 K. Contours represent percentage difference of calculated from measured absorptances for various CO_2 amounts, w, and effective pressures, P_e, for the (*a*) Goody model, (*b*) Malkmus model, (*c*) wide band model.

the assumption of mean Planck function introduces a negligible error of 0.8% in the downward flux at the ground. We therefore adopt (18) and (19) for easy comparison between narrow and wide band fluxes. The narrow band absorptances were calculated for a wave number interval from 500–800 cm^{-1}. For an isothermal temperature profile, (18) and (19) reduce to

$$F^{\uparrow} = \sigma T_s^4 \tag{20}$$

$$F^{\downarrow} = \bar{B}_{15}(T_s)\, A(|u|) \tag{21}$$

The upward flux is just a constant, and the downward flux depends upon the absolute amount of absorptance. Thus, the downward flux is independent of the differencing scheme used in (19).

We have calculated upward and downward fluxes for isothermal and nonisothermal atmospheres for a carbon dioxide concentration of 320 ppm and two times this value using the absorptances of the Goody model, Malkmus model, and the wide band model. Our nonisothermal profiles are taken from *McClatchey et al.* [1971], and they include a tropical, mid-latitude summer and a subarctic winter profile. Because of the neglect of Doppler broadening effects, we limit our flux calculations up to 25 km in altitude.

The downward fluxes for an isothermal atmosphere of 200 K and 300 K are shown in Figures 7*a* to 7*b*, respectively. The pressure levels employed in these calculations are based upon the tropical profile of *McClatchey et al.* [1971]. Shown are the fluxes for the two CO_2 amounts and the three band models. At T = 200 K, the wide band model results are so close to the Goody narrow band model fluxes that we do not show the results on this graph; the Malkmus and Goody model fluxes are in close agreement at all levels. The changes in the fluxes at the surface due to a doubling of CO_2 are 1.09, 1.03, and 1.14 W/m^2 for the Malkmus, Goody and wide band models, respectively. At T = 300 K, the narrow band models are within 1.5 W/m^2 of each other for all levels.

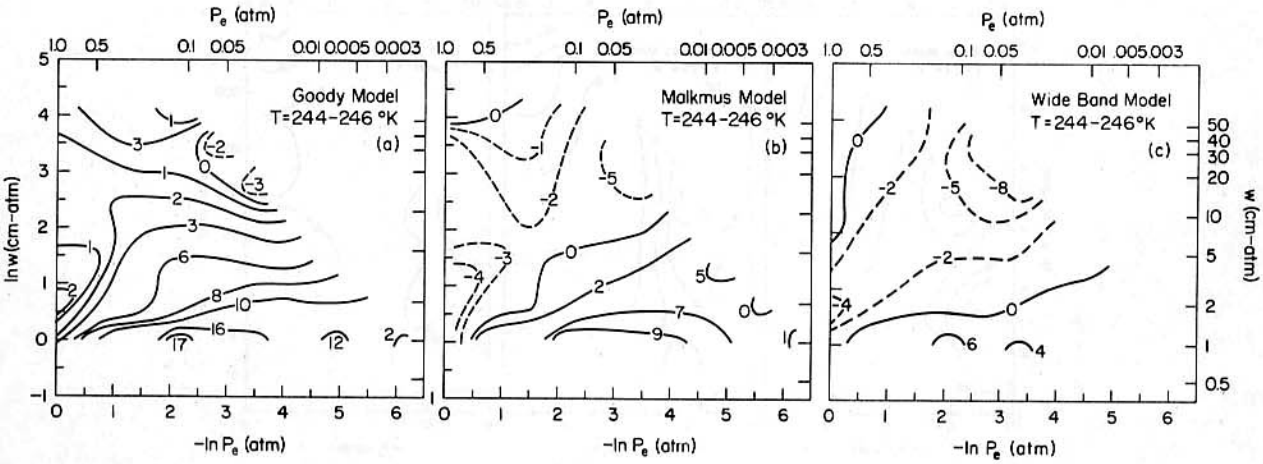

Fig. 5. Comparison of theoretical band absorptances with 24 measured absorptances of *Gryvnak et al.* [1976] for T = 244–246 K. Contours represent percentage difference of calculated from measured absorptances for various CO_2 amounts, w, and effective pressures, P_e, for the (*a*) Goody model, (*b*) Malkmus model, (*c*) wide band model.

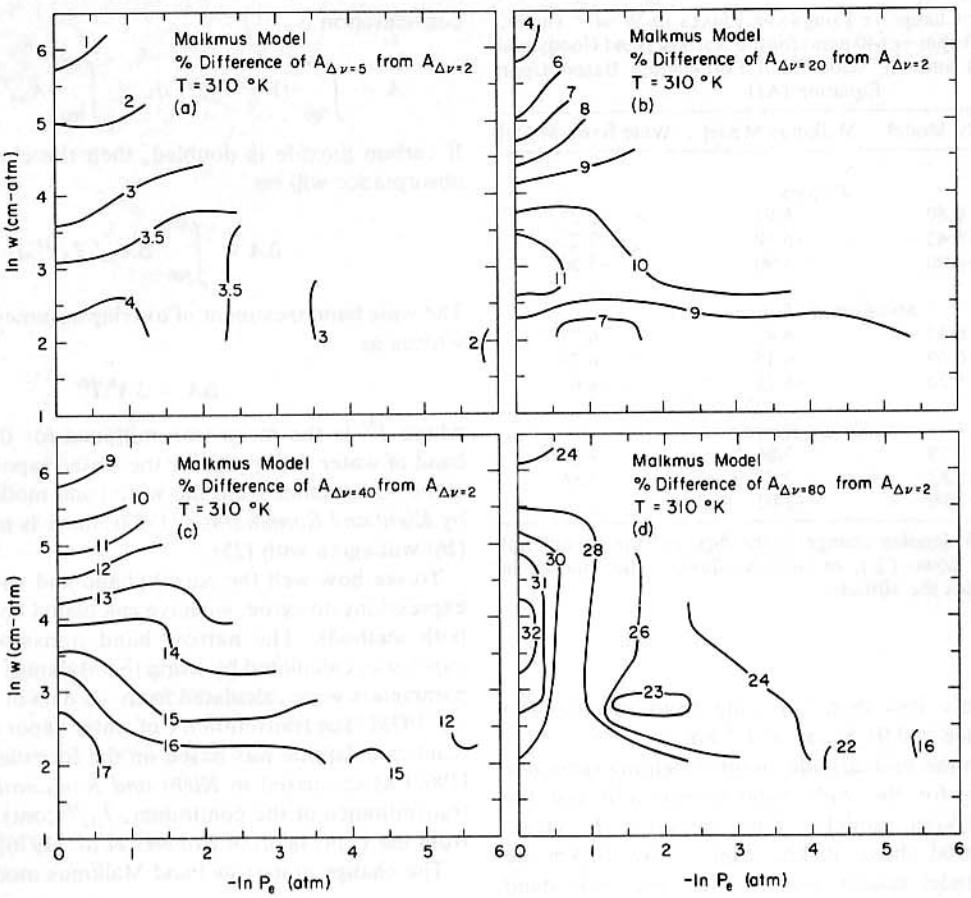

Fig. 6. Dependence of narrow band Malkmus model absorptances upon the spectral interval size, $\Delta\nu$. Contours represent percentage difference of calculated absorptances for a spectral interval of (*a*) 5 cm^{-1}, (*b*) 20 cm^{-1}, (*c*) 40 cm^{-1}, and (*d*) 80 cm^{-1}, with absorptances calculated for $\Delta\nu = 2$ cm^{-1}.

The wide band model fluxes are within 3.0 W/m^2 of those given by the Malkmus model. The changes in the downward flux at the surface due to a doubling of CO_2 are 6.96, 6.98, and 7.10 W/m^2 for the Malkmus, Goody, and wide band models, respectively.

Flux sensitivites for three latitudinal regions and at three levels due to doubling CO_2 for all three models are presented in Table 2. As seen from Table 2 at all levels within the atmosphere, all of the three models agree to within less than 13%.

To evaluate the effect that the size of the spectral interval of the narrow band models has upon the flux sensitivities, we have calculated the change in the net flux, due to doubling CO_2, of the surface-troposphere system for the mid-latitude summer profile for several spectral intervals. Figure 8 shows the change in the net flux for four spectral intervals: 5, 20, 50, and 100 cm^{-1}. Results are shown for both the narrow band models and for the pure CO_2 case, as well as the case of CO_2 overlapped with the pure rotation band of H_2O. These results indicate the substantial errors in the estimated heating with a coarsening of the spectral resolution.

Figure 9*a* represents the change in the tropical heating rates due to doubling CO_2 for the wide band formulation and the narrow band Malkmus model. The two models agree very well above 8 km. Below 8 km, the narrow band model

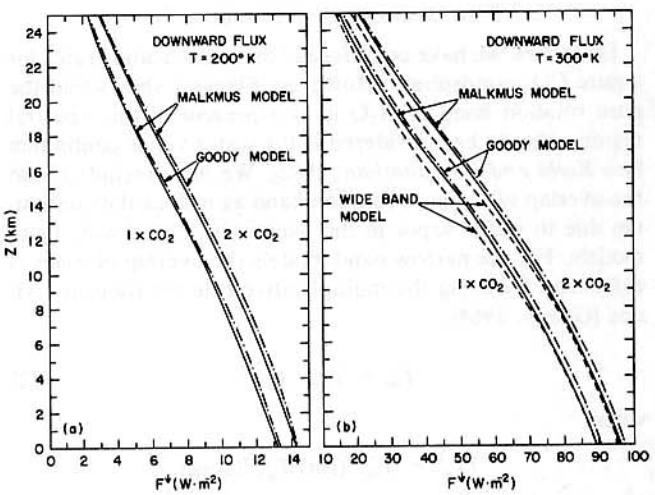

Fig. 7. Downward fluxes due to CO_2, in W/m^2, for an isothermal atmosphere at (*a*) 200 K for the Malkmus model (solid line), and Goody model (dashed-dotted line). Wide band model results are not discernable from Goody model results for this case. Fluxes are for 1 × CO_2, which represents a CO_2 mixing ratio of 320 ppmv, and for 2 × CO_2, and (*b*) 300 K for the Malkmus model (solid line), Goody model (dashed-dotted line), and wide band model (dashed line). Fluxes are for 1 × CO_2, which represents a CO_2 mixing ratio of 320 ppmv, and for 2 × CO_2.

TABLE 2. The Change in Longwave Fluxes in W m^{-2} Due to Doubled CO_2 (320 ppm → 640 ppm) for the Narrow Band Goody and Malkmus Models and the Wide Band Formulation Based Upon Equation (A1)

	Goody Model	Malkmus Model	Wide Band Model
		Tropics	
$\Delta F^{\downarrow}(0)$	6.80	6.85	7.25
$\Delta F^{N}(17)$	−6.43	−6.40	−7.21
$\Delta F^{\uparrow}(25)$	−4.90	−4.90	−5.36
		Mid-latitude Summer	
$\Delta F^{\downarrow}(0)$	6.37	6.42	6.77
$\Delta F^{N}(13)$	−6.09	−6.15	−6.73
$\Delta F^{\uparrow}(25)$	−4.20	−4.22	−4.62
		Subarctic Winter	
$\Delta F^{\downarrow}(0)$	3.79	3.86	4.03
$\Delta F^{N}(8)$	−3.63	−3.72	−3.86
$\Delta F^{\uparrow}(25)$	−2.00	−2.02	−2.24

The symbol ΔF denotes change in the flux and the superscript denotes up ($\uparrow$), down ($\downarrow$), or net (N) fluxes. The number in parentheses denotes the altitude.

heating is slightly less than the wide band results. The greatest difference is 0.01 K/day at 1.5 km.

The change in the mid-latitude summer heating rates due to doubled CO_2 for the wide band formulation and the narrow band Malkmus model is shown in Figure 9*b*. Agreement is fairly good above 10 km, while below 10 km the narrow band model results are less than the wide band results. The greatest difference is only 0.005 K/day at 3.5 km. The change in the subarctic winter heating rates due to doubled CO_2 for the two models is shown in Figure 9*c*. Agreement between the two models is very good below 15 km. Above this height the narrow band model shows greater cooling due to increased CO_2.

5. The Overlap of Absorbing Gases

Up to now we have considered fluxes and heating rates for a pure CO_2 atmosphere. However, Figure 1 shows that the pure rotation band of H_2O is also present in this spectral region. Also to be considered is the water vapor continuum [see *Kiehl and Ramanathan*, 1982]. We have included both the overlap of the pure rotation band as well as the continuum due to water vapor in the narrow band and wide band models. For the narrow band models the overlap of gases is calculated by using the multiplicative rule for transmissivities [*Goody*, 1964],

$$T_{\Delta\nu} = T_{\Delta\nu}{}^{C}\, T_{\Delta\nu}{}^{H} \tag{22}$$

where

$$T_{\Delta\nu}{}^{H} = T_{\Delta\nu}{}^{H}(\text{rot})\, T_{\Delta\nu}{}^{H}(\text{cont})$$

where $T_{\Delta\nu}{}^{C}$, $T_{\Delta\nu}{}^{H}(\text{rot})$, and $T_{\Delta\nu}(\text{cont})$ are the transmissivities of carbon dioxide, the rotation band of water vapor, and the H_2O continuum band for a given spectral interval, $\Delta\nu$, respectively. In terms of absorptivity, (22) becomes

$$A_{\Delta\nu} = 1 - T_{\Delta\nu}{}^{H} + A_{\Delta\nu}{}^{C} T_{\Delta\nu}{}^{H} \tag{23}$$

The total absorptance for the entire spectral region under consideration is

$$A = \int_{500}^{800} \{1 - T_{\Delta\nu}{}^{H}\}\, d\nu + \int_{500}^{800} A_{\Delta\nu}{}^{C} T_{\Delta\nu}{}^{H}\, d\nu \tag{24}$$

If carbon dioxide is doubled, then the change in the total absorptance will be

$$\Delta A = \int_{500}^{800} \Delta A_{\Delta\nu}{}^{C} T_{\Delta\nu}{}^{H}\, d\nu \tag{25}$$

The wide band treatment of overlap assumes that (25) can be written as

$$\Delta A = \Delta A^{C} \bar{T}^{H} \tag{26}$$

where $\bar{T}^{H}$ is the mean transmittance for the pure rotation band of water vapor and for the water vapor continuum. A^{C} is the absorptance from the wide band model. As discussed by *Kiehl and Ramanathan* [1982], there is no guarantee that (26) will agree with (25).

To see how well the narrow band and wide band overlap expressions do agree, we have calculated heating rates using both methods. The narrow band transmissivity of water vapor was calculated by using the Malkmus model. The line parameters were calculated from the data of *McClatchey et al.* [1973]. The transmittance of water vapor used in the wide band calculations was based on the formulation of *Rodgers* [1967] as discussed in *Kiehl and Ramanathan* [1982]. The transmittance of the continuum, $\bar{T}_{\Delta\nu}{}^{H}(\text{cont})$, was calculated from the expression of *Roberts et al.* [1976].

The change in narrow band Malkmus model heating rates

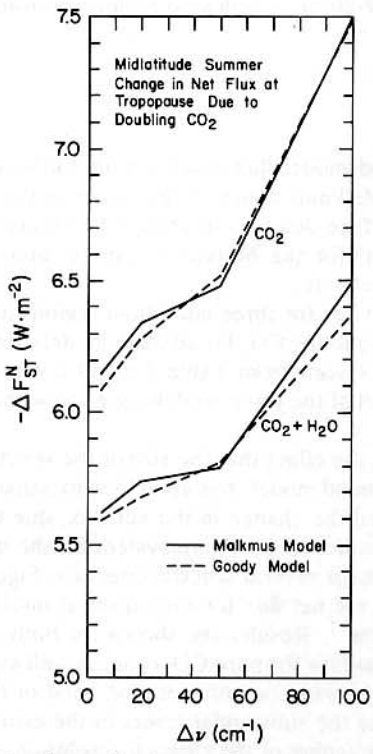

Fig. 8. The change in the net flux at the tropopause due to doubled CO_2 for the mid-latitude summer profile of *McClatchey et al.* [1971] as computed from the narrow band Goody and Malkmus models for various spectral intervals, $\Delta\nu$.

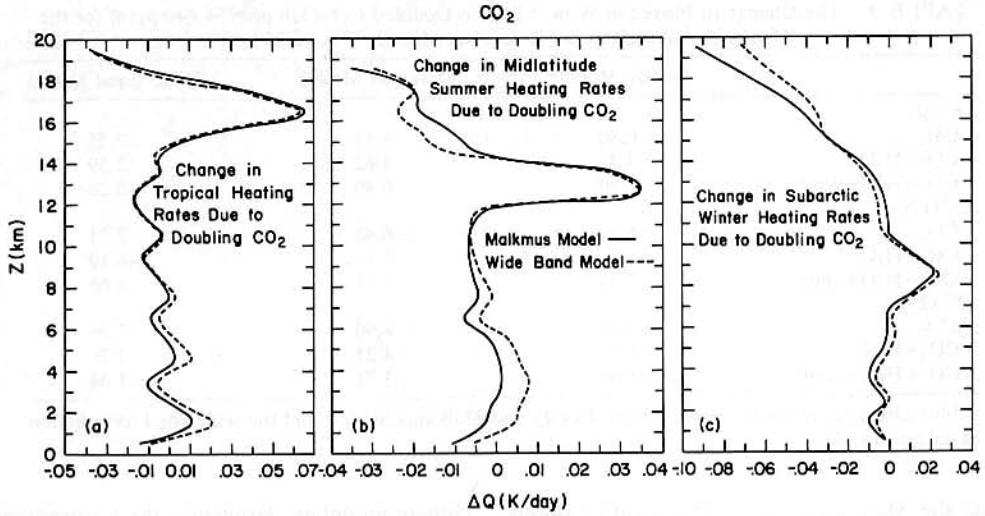

Fig. 9. The change in the CO_2 heating rates due to doubling CO_2, in K/day, for the (*a*) tropical profile, (*b*) mid-latitude summer profile, (*c*) subarctic winter profile of *McClatchey et al.* [1971].

in the tropics due to a doubling of CO_2 for pure CO_2 atmospheres, for CO_2 overlapped by the water vapor rotation band, and for CO_2 overlapped by the water vapor rotation band and the continuum is shown in Figure 10. We see that including the water vapor rotation band has increased the lower tropospheric heating. This is due to water vapor absorbing the increased CO_2 emission. If the continuum is also included, then the heating increases by a factor of over 2 from that of CO_2 plus H_2O. These calculations clearly illustrate the importance of water vapor to tropospheric heating due to increased CO_2.

Flux differences due to doubled CO_2 for the tropical atmosphere which include the water vapor overlap for the three models are presented in Table 3. All of the model results are in good agreement, except for the change in the downward flux at the surface. For this case, the changes in the wide band model flux with overlapped water vapor and continuum differ from the narrow band results by a factor of 1.5. This discrepancy arises from the presence of the water vapor continuum. Although the behavior of the water vapor rotation band exhibits very little regular structure (see Figure 1) in this region, the absorption coefficient of the water vapor continuum decreases monotonically from 500 to 800 cm^{-1}. Thus, the choice of a particular spectral interval size and mean absorption coefficient for the continuum can affect the accuracy of the broad band transmittance of the continuum. To assess the importance of the size of the spectral interval for the continuum transmittance, we have performed Malkmus model calculations with large spectral intervals (>10 cm^{-1}) for the transmittance of the water vapor continuum. We find agreement between the broad band Malkmus model and our broadband model if a large spectral interval is used to evaluate the continuum transmittances. Thus, the presence of the broad band continuum transmittance is the source of discrepancy in the downward flux at the surface, *Ramanathan* [1981] has shown that the surface-tropospheric temperature increase due to increased CO_2 is largely determined by the change in the net flux at the tropopause. Table 3 indicates that all three models are in excellent agreement in calculating this change.

All of the results presented so far have been for clear sky conditions. We have also performed a series of calculations for the tropics which include three cloud layers. The cloud data shown in Table 4 was taken from *Ramanathan and Dickinson* [1979]. The changes in the heating rates due to a doubling of CO_2 for a cloudy tropical atmosphere are shown in Figures 11*a* to 11*c*. The narrow band model results are calculated from the Malkmus model. Agreement between the narrow and the wide band models is very good.

So far we have compared the overlap treatments for the wide band formulation based upon (9) with the narrow band Malkmus model. Because the band model formulations are entirely different, we are not strictly testing whether

$$\int_{500}^{800} A_{\Delta\nu}{}^{C} T_{\Delta\nu}{}^{H}(\text{rot})\, d\nu = A^{C}\bar{T}^{H}(\text{rot}) \tag{27}$$

where A^C and $\bar{T}^H$(rot) were calculated by integrating $A_{\Delta\nu}{}^C$ and $T_{\Delta\nu}{}^H$ over the entire band width, using $\Delta\nu = 5$ cm^{-1}. To test the validity of (27), we have calculated both sides of this

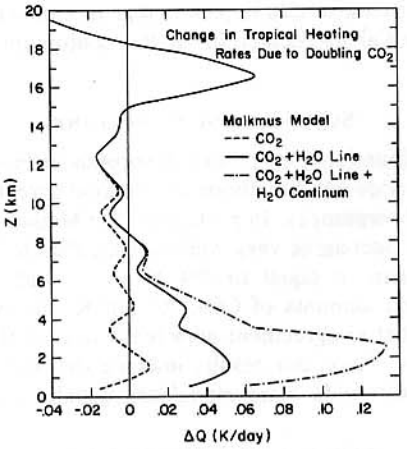

Fig. 10. The change in the narrow band Malkmus model heating rates due to doubling CO_2, in K/day, for the tropical profile of *McClatchey et al.* [1971]. Shown are changes in heating rates for pure CO_2, CO_2 with the pure rotation band of H_2O, and CO_2, pure rotation band of H_2O and the H_2O continuum.

TABLE 3. The Change in Fluxes in W m^{-2} Due to Doubled CO_2 (320 ppm → 640 ppm) for the Tropical Atmosphere at Three Altitudes (0, 17, and 25 km)

	Goody Model	Malkmus Model	Wide Band Model
$\Delta F^{\downarrow}(0)$			
CO_2	6.80	6.85	7.25
CO_2+H_2O	3.53	3.62	2.59
CO_2+H_2O+cont.	0.40	0.40	0.26
$\Delta F^{N}(17)$			
CO_2	−6.43	−6.40	−7.21
CO_2+H_2O	−5.81	−5.87	−6.10
CO_2+H_2O+cont.	−5.33	−5.38	−5.66
$\Delta F^{\uparrow}(25)$			
CO_2	−4.90	−4.90	−5.36
CO_2+H_2O	−4.13	−4.21	−4.26
CO_2+H_2O+cont.	−3.65	−3.71	−3.84

Flux changes are for the narrow band Goody and Malkmus models and the wide band formulation based upon (A1).

expression using the Malkmus model. The greatest difference between the narrow band approach, the left-hand side of (27), and the wide band approach, the right-hand side of the equation, occurs for a path length extending from the top of a tropical atmosphere to the surface. For this case, the wide band approach is about 5% less than the narrow band approach. For stratospheric path lengths the difference is −0.1%. To see how these two methods affect radiative fluxes, we have calculated the upward and downward fluxes for three representative latitudes using the narrow and wide band methods of (27). The percent difference between the wide band and narrow band Malkmus model upward and downward fluxes, respectively, for the tropics, mid-latitude summer, and subarctic winter profiles of *McClatchey et al.* [1971] are shown in Figure 12. The downward flux at the surface for the wide band model is less than the narrow band flux by 4.5%. This difference decreases for higher latitudes due to the smaller water vapor amounts. Above 12 km there is little difference between the narrow and the wide band overlap approaches. There is very little difference between the two approaches for the upward fluxes at any latitude. We point out that these calculations do not include the water vapor continuum. If the continuum is included, then substantial differences in the calculated fluxes near the surface, where water vapor partial pressures are greatest, may arise. The source of these differences is due to choosing a large spectral interval for evaluation of the continuum transmittances.

6. SUMMARY AND CONCLUSIONS

We have found that calculated absorptances based on the narrow and wide band methods are in good agreement with measured absorptances. In particular, the Malkmus and the wide band model agree very well with the data for temperatures less than or equal to 294 K and a wide range of pressures and amounts of CO_2. At 310 K, the wide band model is in better agreement with the data than the narrow band models. Thus, our results indicate that the Malkmus model and the wide band model are equally suitable for climate modeling. However, the accuracy of the wide band model depends crucially on the details of the bands included in the model. The wide band model used in this study facilitates the inclusion of hot and isotopic bands and yields excellent agreement with narrow band models and measurements. However, if we construct a wide band model by coarsening the resolution of the Goody or Malkmus narrow band model, then poor agreement with measured and higher resolution calculations results. Hence, great care should be exercised in constructing wide band models that explicitly account for hot and isotopic bands.

TABLE 4. Tropical Cloud Data

Type	Height, km	Fractional Amount	Emissivity
Low	2	0.22	1.0
Middle	6	0.08	1.0
High	10	0.19	0.5

The upward and downward directed fluxes for both narrow and wide band models for both nonisothermal and isothermal conditions are in very good agreement with each other. More importantly, the sensitivity of these fluxes due to a doubling of CO_2 are in agreement. In particular, we find that the change in the surface-troposphere fluxes for the narrow and wide band models agree to within less than 13%. Clear-sky heating rates for a pure CO_2 atmosphere indicate that the two methods are in excellent agreement above the tropopause. Below the tropopause, the wide band method exhibits slightly larger heating rates than the narrow band method.

To investigate the importance of the overlap of absorber gases, we have included in our calculations the rotation band of H_2O as well as the water vapor continuum. We find very little difference between the narrow and the wide band approaches to the overlap problem. In particular, the change in surface-troposphere fluxes for the two methods due to a doubling of CO_2 agree to within less than 5%. However, the change in the downward flux at the surface due to doubling of CO_2 for the wide band model is smaller than the narrow band result. If the Malkmus model is used for both narrow and wide band overlap calculations between CO_2 and the pure rotation band of water vapor, then a maximum difference of 4.5% between these two approaches occurs for the tropical case for the downward flux at the surface. However, we find that the overlap effect of the water vapor continuum with CO_2 bands is sensitive to the size of the interval employed in its formulation.

On the basis of the results of this study, we conclude that narrow and wide band models are equally suitable for use in climate models. Since the flux sensitivities to CO_2 increase as computed by these two methods are in good agreement with one another, we would expect differences in model response, due to a doubling of CO_2, to be minimal. This

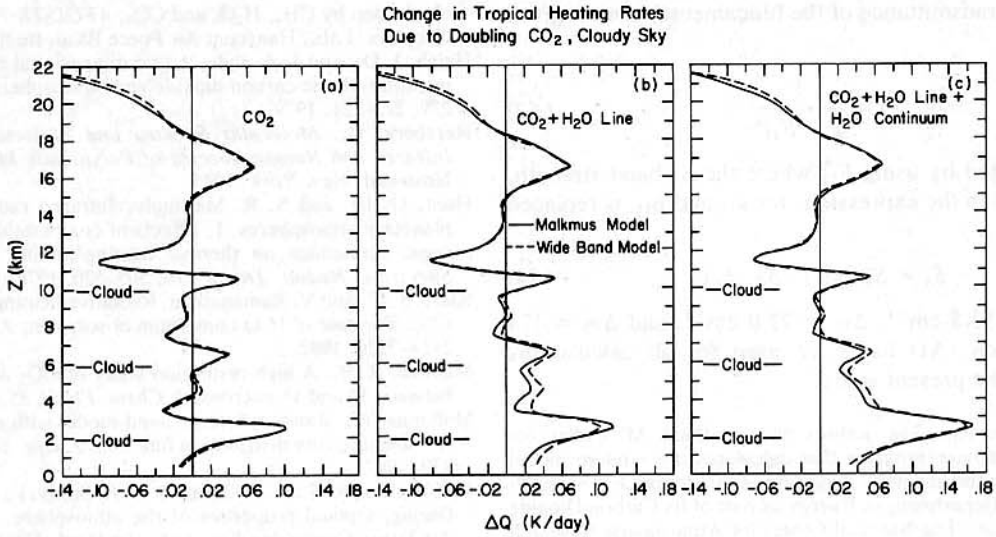

Fig. 11. The change in the cloudy sky heating rates due to doubling CO_2, in K/day, for the (*a*) tropical profile, (*b*) mid-latitude summer profile, (*c*) subarctic winter profile of *McClatchey et al.* [1971].

conclusion, however, is based upon comparing a narrow band model that employs a spectral interval of 5 cm^{-1}. We have shown that larger intervals can lead to large disagreement with measured absorptances. Hence, we find the optimal spectral interval for the narrow band model, for the 15-μm CO_2 band system, to be on the order of 5 cm^{-1}. If this size interval is employed, then the narrow band models are in good agreement with measured absorptances and the wide band model used in this study.

Finally, we illustrate the effect of H_2O overlap on increased CO_2 heating rates. We find that H_2O absorption of increased CO_2 emission significantly enhances heating of the lower troposphere (see Figure 10), but that the overall effect on the heating of the surface-troposphere system is small.

APPENDIX

As mentioned in section 2.2, the expression for the total band absorptance given by (9) implicitly assumes that all vibrational bands are completely overlapped. Inspection of Table 1 indicates, however, that some bands are separated by more than 40 cm^{-1}. Thus, equation (9) must be modified to account for this band structure. *Ramanathan* [1976] has shown how band separation effects can be incorporated into the present formulation. The bands, which are not completely overlapped, are numbers 3 and 13, 2 and 14, 6, 7, 8, 10. We assume that bands 3 and 13, as well as 2 and 14, are completely overlapped. The total absorptance according to *Ramanathan* [1976] is

$$A = 2A_0 \ln\left[1 + \sum_{i=1}^{4} (F_{i1} + F_{i4} + F_{i5} + F_{i9} + F_{i11} + F_{i12})\right]$$

$$+ T_1 \ln\left[1 + \sum_{i=1}^{4} (F_{i2} + F_{i14})\right]$$

$$+ T_1 \ln\left[1 + \sum_{i=1}^{4} (F_{i3} + F_{i13})\right]$$

$$+ T_2 \ln\left[1 + \sum_{i=1}^{4} F_{i7}\right] + T_2 \ln\left[1 + \sum_{i=1}^{4} F_{i8}\right]$$

$$+ T_3 \ln\left[1 + \sum_{i=1}^{4} F_{i10}\right] + T_3 \ln\left[1 + \sum_{i=1}^{4} F_{i6}\right] \quad \text{(A1)}$$

where

$$F_{ij} = \frac{u_{ij}}{[4 + u_{ij}(1 + 1/\beta_{ij})]^{1/2}} \quad \text{(A2)}$$

u_{ij} and β_{ij} are defined by (10) and (11), respectively. T_1, T_2, and T_3 account for the partial overlap between the fundamental band and those bands that are not completely over-

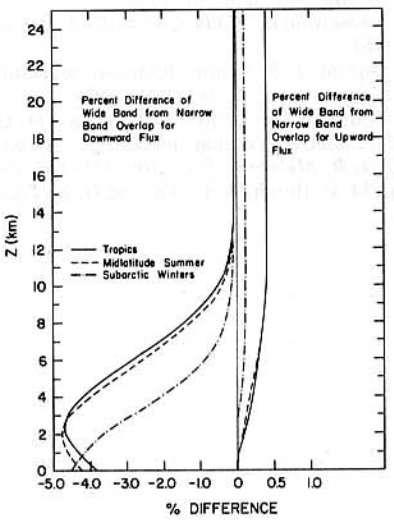

Fig. 12. Percent difference of the Malkmus model wide band overlap treatment from the narrow band overlap treatment in upward and downward fluxes for the tropical (solid line), mid-latitude summer (dashed line), and subarctic winter (dashed-dotted line) profiles.

lapped. This transmittance of the fundamental band is given by

$$T_k = \frac{1}{1 + \bar{F}_{11}{}^k} \tag{A3}$$

$\bar{F}_{11}{}^k$ is evaluated by using F_{11} where the S_1 band strength, which appears in the expressions for u_{11} and β_{11}, is replaced by

$$\bar{S}_1 = S_1 \exp(-\Delta\nu_k/A_0) \tag{A4}$$

where $\Delta\nu_1 = 53.5$ cm^{-1}, $\Delta\nu_2 = 72.0$ cm^{-1}, and $\Delta\nu_3 = 124$ cm^{-1}. Equation (A1) has been used for all calculations employed in the present study.

Acknowledgments. The authors wish to thank M. Coffey for giving us a computer program that calculates the random model parameters from the line data. A portion of this research is supported by the U.S. Department of Energy as part of its Carbon Dioxide Research Program. The National Center for Atmospheric Research is sponsored by the National Science Foundation.

REFERENCES

Burch, D. E., D. A. Gryvnak, and D. Williams, Total absorptance of carbon dioxide in the infrared, *Appl. Opt.*, *1*, 759–765, 1962.

Cess, R. D., and V. Ramanathan, Radiative transfer in the atmosphere of Mars and that of Venus above the cloud deck, *J. Quant. Spectrosc. Radiat. Transf.*, *12*, 933–945, 1972.

Cess, R. D., and S. N. Tiwari, Infrared radiative energy transfer in gases, *Adv. Heat Transf.*, *8*, 229–283, 1972.

Drayson, S. R., A listing of wavenumbers and intensities of carbon dioxide absorption lines between 12 and 20 μm, *Rep 036350-4-T*, Univ. of Mich., Ann Arbor, 1973.

Edwards, D. K., Absorption by infrared bands of carbon dioxide gas at elevated pressures and temperatures, *J. Opt. Soc. Am.*, *50*, 617–626, 1960.

Edwards, D. K., and W. A. Menard, Comparison of models for correlation of total band absorption, *Appl. Opt.*, *3*, 621–625, 1964.

Ellingson, R. G., and J. C. Gille, An infrared radiative transfer model, 1, Model description and comparison of observations with calculations, *J. Atmos. Sci.*, *35*, 523–545, 1978.

Gille, J. C., Methods of Calculating infrared transfer—A review, in *Proceedings, UCLA International Conference on Radiation and Remote Probing of the Atmosphere*, edited by J. G. Kuriyan, University of California, Los Angeles, 1973.

Goody, R. M., A statistical model for water-vapour absorption, *Q. J. R. Meteorol. Soc.*, *78*, 165–169, 1952.

Goody, R. M., *Atmospheric Radiation*, Oxford University Press, New York, 1964.

Goody, R. M., and M. J. S. Belton, Radiative relaxation times for Mars, *Planet. Space Sci.*, *15*, 247–256, 1967.

Groves, K. S., and A. F. Tuck, Stratospheric O_3-CO_2 coupling in a photochemical-radiative column model, 1, Without chlorine chemistry, *Q. J. R. Meteorol. Soc.*, *106*, 125–140, 1980.

Gryvnak, D. A., D. E. Burch, R. L. Alt, and D. K. Zgonc, Infrared absorption by CH_4, H_2O, and CO_2, *AFGL-TR-76-0246*, Air Force Geophys. Lab., Hanscom Air Force Base, Bedford, Mass., 1976.

Haigh, J. D., and J. A. Pyle, A two-dimensional calculation including atmospheric carbon dioxide and stratospheric ozone, *Nature*, *279*, 222–224, 1979.

Herzberg, G., *Molecular Spectra and Molecular Structure*, 2, *Infrared and Raman Spectra of Polyatomic Molecules*, D. Van Nostrand, New York, 1945.

Hunt, G. E., and S. R. Mattingly, Infrared radiative transfer in planetary atmospheres, 1, Effects of computational and spectroscopic economics on thermal heating/cooling rates, *J. Quant. Spectrosc. Radiat. Transf.*, *16*, 505–520, 1976.

Kiehl, J. T., and V. Ramanathan, Radiative heating due to increased CO_2: The role of H_2O continuum absorption, *J. Atmos. Sci.*, *39*, 2923–2926, 1982.

Madden, R. P., A high-resolution study of CO_2 absorption spectra between 15 and 18 microns, *J. Chem. Phys.*, *35*, 2083–2097, 1961.

Malkmus, W., Random lorentz band model with exponential-tailed S^{-1} line intensity distribution function, *J. Opt. Soc. Am.*, *57*, 323–329, 1967.

McClatchey, R. S., R. W. Fenn, J. E. A. Selby, F. E. Volz, and J. S. Garing, Optical properties of the atmosphere, *AFCRL-71-0279*, Air Force Cambridge Res. Lab., Bedford, Mass., 1971.

McClatchey, R. S., W. S. Benedict, S. A. Clough, D. E. Burch, R. F. Calfee, K. Fox, J. S. Garing, and L. S. Rothman, AFCRL atmospheric absorption line parameters compilation, *AFCRL-TR-73-0096*, Air Force Cambridge Res. Lab., Bedford, Mass., 1973.

Penner, S. S., *Quantitative Molecular Spectroscopy and Gas Emissivities*, p. 587, Addison-Wesley, New York, 1959.

Ramanathan, V., Radiative transfer within the earth's troposphere and stratosphere: A simplified radiative-convective model, *J. Atmos. Sci.*, *33*, 1330–1346, 1976.

Ramanathan, V., and R. E. Dickinson, The role of stratospheric ozone in the zonal and seasonal radiative energy balance of the earth-troposphere systems, *J. Atmos. Sci.*, *36*, 1084–1104, 1979.

Ramanathan, V., The role of ocean-atmosphere interactions in the CO_2 climate problem, *J. Atmos. Sci.*, *38*, 918–930, 1981.

Roberts, R. E., J. E. A. Selby, and L. M. Biberman, Infrared continuum absorption by atmospheric water vapor in the 8–12 μm window, *Appl. Opt.*, *15*, 2085–2090, 1976.

Robertson, D. C., L. S. Bernstein, R. Haimes, J. Wunderlich, and L. Vega, 5 cm^{-1} band model option to LOWTRAN5, *Appl. Opt.*, *20*, 3218–3226, 1981.

Rodgers, C. D., The use of emissivity in atmospheric radiation calculations, *Q. J. R. Meteorol. Soc.*, *93*, 43–54, 1967.

Rodgers, C. D., and C. D. Walshaw, The computation of infrared cooling rate in planetary atmosphere, *Q. J. R. Meteorol. Soc.*, *92*, 67–92, 1966.

Yamamoto, G., and T. Sasamori, Numerical study of water vapor transmission, *Geophysics*, *8*, 36–45, 1957.

Yamamoto, G., M. Tanaka, and T. Aoki, Estimation of rotational line widths of carbon dioxide bands, *J. Quant. Spectrosc. Radiat. Transf.*, *9*, 371–382, 1969.

(Received August 2, 1982;
revised February 18, 1983;
accepted February 28, 1983.)